



# The eruption in Fagradalsfjall (2021, Iceland): how the operational monitoring and the volcanic hazard assessment contributed to its safe access

S. Barsotti<sup>1</sup> · M. M. Parks<sup>1</sup> · M. A. Pfeffer<sup>1</sup> · B. A. Óladóttir<sup>1</sup> · T. Barnie<sup>1</sup> ·  
M. M. Titos<sup>1,5</sup> · K. Jónsdóttir<sup>1</sup> · G. B. M. Pedersen<sup>2</sup> · Á. R. Hjartardóttir<sup>2</sup> ·  
G. Stefansdóttir<sup>1</sup> · T. Johannsson<sup>3</sup> · Þ. Arason<sup>1</sup> · M. T. Gudmundsson<sup>2</sup> ·  
B. Oddsson<sup>4</sup> · R. H. Þrastarson<sup>1</sup> · B. G. Ófeigsson<sup>1</sup> · K. Vogfjörð<sup>1</sup> · H. Geirsson<sup>2</sup> ·  
T. Hjörvar<sup>1</sup> · S. von Löwis<sup>1</sup> · G. N. Petersen<sup>1</sup> · E. M. Sigurðsson<sup>1</sup>

Received: 15 March 2022 / Accepted: 20 December 2022 / Published online: 7 January 2023  
© The Author(s) 2023

## Abstract

After more than a year of unrest, a small effusive eruption commenced in Fagradalsfjall, Iceland, on 19 March 2021. The eruption lasted six months. The first six weeks were characterized by multiple fissure openings, and the remainder was dominated by effusive activity from a single crater. During the eruption, lava and low-level gases propagated over the complex terrain: a hyaloclastite massif with mountain peaks up to about 350 m asl with valleys in between. The area is uninhabited, but easily accessible at about 30 km distance from Reykjavík. While the eruption was ongoing, more than 356,000 tourists visited the eruptive site. To maintain low risk access to the area, it was critical to monitor the eruption (including opening of new fissures) in real-time, forecast the transport of gas and lava flow emplacement, and assess the evolving hazards. In addition to data accessibility and interpretation, managing this volcanic crisis was possible thanks to strong collaboration between the scientific institutions and civil protection agencies. The eruption presented an opportunity to tune, test and validate a variety of numerical models for hazard assessment as well as to refine and improve the delivery of information to the general public, communities living near the eruption site and decision makers. The monitoring team worked long hours during both the pre- and syn-eruptive phases for identifying low risk access areas to the eruption site and to provide a regular flow of information. This paper reviews the eruption and its associated hazards. It also provides an overview of the monitoring setup, the adopted numerical tools and communication materials disseminated to the general public regarding current exclusion zones, hazards and possible future eruptive scenarios.

**Keywords** Fagradalsfjall eruption · Low risk access · Operational response · Volcanic hazards · Eruption monitoring · Tourism

---

✉ S. Barsotti  
sara@vedur.is

Extended author information available on the last page of the article

## 1 Introduction

There is on average an eruption every 3–5 years in Iceland (Gudmundsson et al. 2008). Prior to the 2021 Fagradalsfjall event, the last eruption occurred in 2014–2015 at Bárðarbunga volcano (Barsotti et al. 2020a, 2020b; Gudmundsson et al. 2016; Sigmundsson et al. 2015). As such, while the timing of the Fagradalsfjall eruption was not surprising, the location was unexpected: the last eruption within the Reykjanes Peninsula occurred nearly 800 years prior (Sæmundsson et al. 2020).

The Reykjanes Peninsula is the on-shore continuation of the Mid-Atlantic Reykjanes ridge. The Peninsula comprises five main volcanic systems, from west to east: Reykjanes, Svartsengi, Fagradalsfjall, Krýsuvík, and Brennisteinsfjöll (see Fig. 1). These systems are characterized by numerous strike-slip and normal faults, historic eruptive fissures and post-glacial lava flows. Along the Peninsula an array of adjacent N-S aligned strike-slip faults accommodate the shearing motion of the oblique Reykjanes rift (Clifton and Kattenhorn 2006; Sæmundsson 1978). Fagradalsfjall is defined as an embryonic volcanic system as it has no associated geothermal activity and it lacks a fissure swarm (Sæmundsson et al. 2020). For this reason, it had previously been considered a part of the neighbouring Krýsuvík volcanic system (Einarsson 2019).

While earthquake activity is relatively high on the Peninsula (e.g. Björnsson et al. 2020; Clifton and Kattenhorn 2006; Einarsson 1991), eruptive activity is infrequent, occurring at intervals of 800–1000 years (Sæmundsson et al. 2020). However, the eruptive periods may last from few decades to ~500 years, comprising intermittent

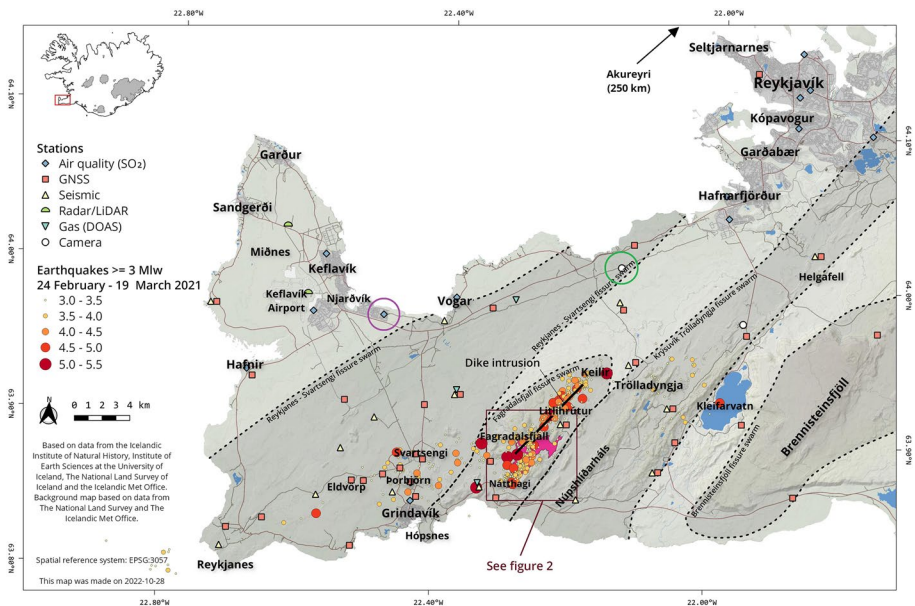


**Fig. 1** The Reykjanes Peninsula, the location of earthquakes above M3 for the period from 24 February to 19 March 2021 (coloured filled circles), the dyke intrusion as mapped by InSAR images (black line), the final Fagradalsfjall lava field extent (pink polygon), and the extent of the detailed map (see Fig. 2, red outline). The volcanic systems which belong to the Reykjanes peninsula are marked as grey areas. Monitoring stations are shown with different symbols. Key sites mentioned in the text are identified with a large open circle. Key locations mentioned in the text are also included

eruptions (Sæmundsson and Sigurgeirsson 2013). These eruptions are generally effusive, although minor ash has been produced. On the Peninsula, the Fagradalsfjall volcanic system appears to have been the least active during postglacial times. The last prior eruption occurred over 6000 years ago and the system also has fewer faults and eruptions compared to the other volcanic systems. It was not active during the last three volcanic episodes in the area, during which all the other volcanic systems became activated (Sæmundsson et al. 2020).

The Reykjanes Peninsula entered a period of volcano-tectonic unrest more than one year prior to the eruption. Seismic and intrusive activity caused clear geophysical signals a few weeks before the eruption, enabling the Icelandic Meteorological Office (IMO), together with colleagues at the University of Iceland (UI), Environment Agency of Iceland (EAI), the Iceland GeoSurvey (ÍSOR), the Icelandic Institute of Natural History and the Department of Civil Protection and Emergency Management of the National Commissioner of the Icelandic Police (CP), to prepare for a possible escalation of events.

Successful volcanic eruption management requires preparation, interpretation of monitoring data and effective communication (Lowenstern et al. 2022; Pallister et al. 2019). These elements can be challenging, especially if the volcano has not erupted in modern times and if the site rapidly becomes a popular touristic attraction (Gaudru 2014). The capability to determine possible eruptive scenarios depends largely on the amount and quality of available data, including access to detailed geological maps and information concerning previous eruptions and episodes of unrest. There is added complexity when there is also uncertainty regarding the location of possible fissure and vent openings. This is the case for the Icelandic volcanic systems, where an eruption can originate from a fissure anywhere within an area that can be hundreds of kilometres long and tens of kilometres wide (Gudmundsson et al. 2008).

Throughout the period of the 2019–2021 volcanic unrest, the Fagradalsfjall volcanic system was categorized as a part of the Krýsuvík volcanic system. It was elevated to a yellow aviation colour code (following the International Civil Aviation Organization standards, ICAO 2020) on 24 February 2021, when an earthquake of magnitude M5.6 shook the Reykjanes Peninsula, and GNSS stations in the area began to show rapid deformation on a daily basis, marking the onset of a dyke intrusion within the Fagradalsfjall region (Sigmundsson et al. 2022). At this time the Scientific Advisory Board, a consortium of experts from Icelandic agencies (including representatives from agencies already mentioned), was activated by the CP and convened regularly to: (1) understand and interpret the underlying processes and (2) identify and rank likelihood of possible scenarios. The most likely eruptive scenario, based on past eruptive activity and mapped volcanic products (Einarsson 2019; Sæmundsson et al. 2020), was identified to be an effusive eruption with release of volcanic gases into the atmosphere. Therefore, the most likely hazards would be lava flows near the vent area and gases potentially impacting air quality in both the near and far field. At this time the location(s) of potential fissure openings remained uncertain as the data was indicating that a segmented dike was continuing to propagate. The final length of the dike was approximately 9 km (see Fig. 1) and comprised two segments—the northern segment striking at N45°E and the southern segment at approximately N24°E (Sigmundsson et al. 2022). The preparatory work that followed focused on the area that was at that time affected by elevated seismicity and deformation. Lessons learnt from the Bárðarbunga eruption (Barsotti et al. 2020a, 2020b; Ilyinskaya et al. 2017; Pfeffer et al. 2018) provided, for example, a basis for how to implement a monitoring and forecasting system for lava flows and volcanic gas hazards.

The proximity of the active area to Reykjavík and the international airport emphasized the need for enhanced monitoring and it also facilitated access to the area.

From the start of the eruption on 19 March 2021 at 20:30 UTC, four main eruptive phases were identified based on different source locations, eruptive styles, magma extrusion rates, SO<sub>2</sub> fluxes and associated hazards. The eruption was declared over on 18 December, with the last active lava flows detected on 18 September (Icelandic Meteorological Office 2022). A second short-lived eruption occurred during Summer 2022 (3–21 August), just one km NE of the eruption site in Geldinagadalir.

This paper provides an overview of the course of the events during the 2021 eruption, the short-term to real-time hazard assessments performed and the communication of these findings. Our combined efforts provided low risk access and protected viewing spots, ensuring a protected and rewarding experience for the hundreds of thousands of people who came to view the eruption.

## 2 Background activity and the unrest phase

The Reykjanes Peninsula, while very geodynamically active, has been a volcanically quiet area for hundreds of years. The Reykjanes Peninsula has been instrumentally monitored since the 1960s when the first precise distance measurements were done, and levelling profiles measured (Brander et al. 1976; Tryggvason 1970). The first seismometers (part of the nascent Icelandic seismic network) were installed in the 1970s (Björnsson et al. 2020; Klein et al. 1973, 1977), followed by Global Positioning System (GPS) campaign measurements which started in the 1980s (Foulger et al. 1987; Hreinsdóttir et al. 2001; Sturkell et al. 1994, 2006).

Seismicity, mainly on strike-slip faults, has been consistently detected on the Peninsula, although it occurs episodically (Björnsson et al. 2020; Einarsson 2008). Global Navigation Satellite System (GNSS) observations along the Peninsula reveal that most of the deformation related to plate-spreading on Reykjanes is taking place in the southern and central part of the Peninsula, whereas less deformation is occurring in the northern part (Sigmundsson et al. 2020). A overall subsidence trend has previously been observed along the Peninsula (Árnadóttir et al. 2009) with localized subsidence in the vicinity of powerplants (due to geothermal extraction) and several inflation events (attributed to pressurization of hydrothermal reservoirs) which were observed during the past decades (Geirsson et al. 2010; Hreinsdóttir et al. 2001; Keiding et al. 2010). The level of seismic activity and deformation characterizing the unrest which led up to the 2021 Fagradalsfjall eruption had never before been detected on the Peninsula, since the start of instrumental recordings in Iceland.

Intense seismicity and ground deformation was observed during a 14-month long period of volcano-tectonic unrest along the Reykjanes Peninsula, suggesting that a large portion of the Peninsula had reactivated. This unrest phase preceded both the pre-eruptive dyke intrusion and the eventual eruption at Fagradalsfjall (Fig. 1).

Increased seismicity was initially detected in December 2019 in the Fagradalsfjall region. A seismic swarm initially occurred between 15 and 20 December 2019, comprising about 500 earthquakes >M1. These earthquakes were located at depths between 3 and 7 km, with two apparent trends—one N-S and the other E-W. This seismicity was followed by about 2 months of quiescence. On 21 January 2020 activity re-commenced on the Peninsula, with a small cluster of earthquakes detected near

Grindavík town (10 km southwest of the previous earthquakes). On 22 January the earthquake activity increased, with about 100 earthquakes 5 km west of Fagradalsfjall (three  $\geq$  M3).

Concurrently, deformation was detected at two cGNSS stations in this area (Svartsengi-Þorbjörn region) and verified by interferometric analysis of Sentinel-1 satellite images. Geodetic modelling of these observations indicated that the observed deformation was due to a pressure increase within the shallow crust directly west of Mt. Þorbjörn within the Reykjanes-Svartsengi volcanic system (unpublished geodetic modelling) (Fig. 1). The geodetic inversion results indicated the most likely cause of the seismic and deformation changes was the intrusion of a magmatic sill at a depth of about 4 km, corresponding to a volume change of  $\sim 3$  million  $\text{m}^3$ . A plan for enhanced monitoring of the Reykjanes Peninsula was subsequently implemented: (1) three additional cGNSS instruments and one additional seismometer were installed in the area, (2) data from the seismic instruments operated by ÍSOR and Czech Academy of Sciences were integrated into the IMO real-time processing and monitoring system, and (3) the frequency of gas measurements at high-temperature geothermal areas on the Reykjanes Peninsula was increased, including at Svartsengi, Eldvörp, Gunnuhver, and Seltún.

The initial intrusion detected in January 2020 near Mt. Þorbjörn was followed by two additional sill-type intrusions at the same location. These were intruded between 6 March–17 April, and 15 May–22 July 2020. The three intrusions in the vicinity of Svartsengi -Mt Þorbjörn were located at similar depths at about 3–4 km, had similar geometries and comprised a total volume change of about 9 million  $\text{m}^3$ . In addition, temporal seismic velocity changes were detected between January and July 2020 at Mt. Þorbjörn-Svartsengi, Iceland, using seismic ambient noise, signifying crustal changes likely due to crack opening (Cubuk-Sabuncu et al. 2021). In mid-July 2020 a fourth inflation event was detected on the Reykjanes Peninsula, this time in the Krýsuvík volcanic system to the East of Fagradalsfjall. This last episode lasted six months and geodetic inversions of both cGNSS and InSAR observations indicated that the deformation was produced by a combination of a deflating sill-like source at a depth of  $\sim 16$  km and inflation of a body at a depth of  $\sim 6$  km.

During the period of unrest from December 2019 to February 2021, seismicity switched on and off along various regions across the Peninsula, in relation to a combination of processes—intrusions, triggered seismicity and background tectonic activity. Almost 7000 earthquakes  $> M1$  were detected across a 40 km long segment between the westernmost tip of Reykjanes and Kleifarvatn (see Fig. 1). By this time, it was evident that the reactivation of the Peninsula was most triggered by magma inflow and emplacement of shallow-mid crustal magma bodies at multiple locations along the Peninsula.

A M5.6 earthquake shook the Reykjanes Peninsula on 24 February 2021 at 10.05 UTC, marking a new phase in activity with the onset of a dyke propagation in the vicinity of Fagradalsfjall. This was characterized by even more intense seismic swarms extending over a much larger area than before. During the first 24 h,  $\sim 1000$  earthquakes with magnitude  $1 \leq M \leq 3$  and  $\sim 70$  larger than M3 were automatically detected. This seismic activity was occurring not only in the region of emplacement, but extending west to Svartsengi (along the plate boundary) and east to Krýsuvík geothermal area. This dyke was intruded over a period of three weeks and comprised multiple segments, with a total length of about 9 km, extending from south of Keilir to Lyngbrekkur (see Fig. 1). Geodetic inversions of GNSS and InSAR observations indicated a total intruded volume of about 30 million  $\text{m}^3$  (Sigmundsson et al. 2022), substantially larger than the

previous intrusions in 2020. This intrusion culminated in an effusive eruption which commenced on 19 March 2021 at 20:30 UTC.

### 3 Operational geophysical and atmospheric monitoring setup

A variety of sensors and instruments were installed to stream data to IMO, the Volcano Observatory in Iceland, to follow changes in activity (Figs. 1 and 2). In addition to these data streams, complementary monitoring resources were made available through long lasting collaboration between the institutions involved in volcanic crisis response and included information/observations/data available at different temporal frequencies. Some

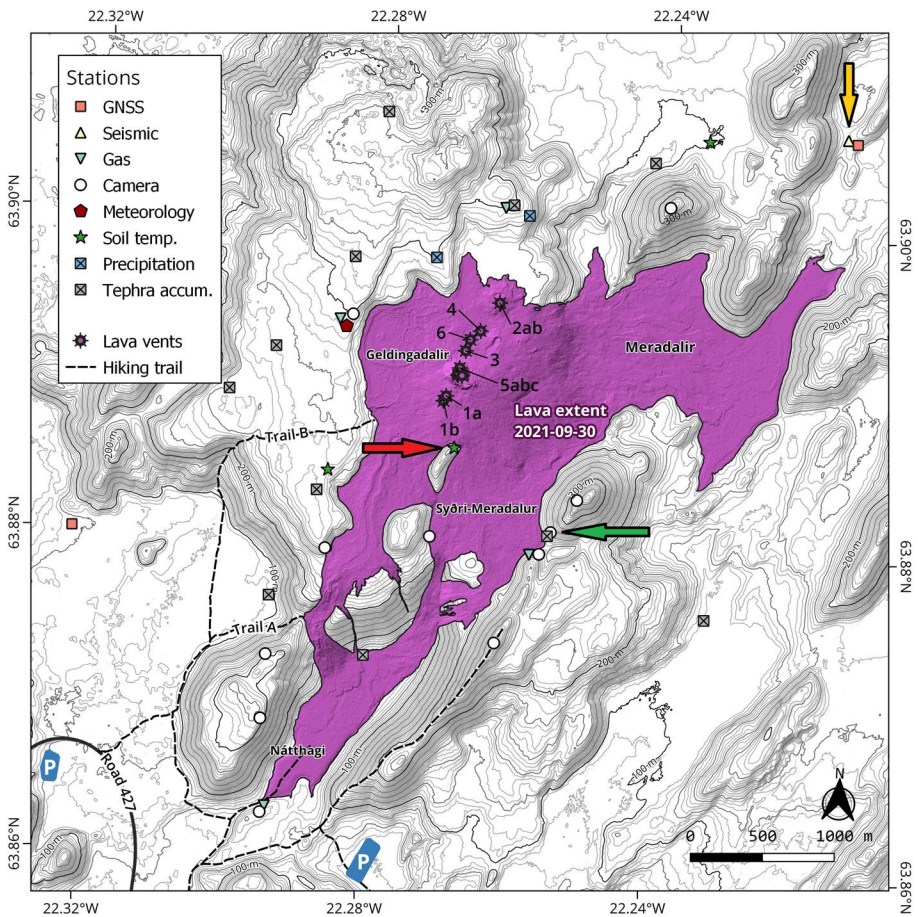


**Fig. 2** A detailed map of the eruption site showing the location of monitoring instrumentation around the eruption site (different stations are marked with different symbols). The final extension of the lava field at the end of the eruption is mapped in purple (survey performed on 30 September 2021, Pedersen et al. 2021). Footpath and hiking trails are indicated as dashed lines, and two of the parking lots are showed and marked with P. The nine lava vents are showed as stars. Coloured arrows point to monitoring sites referred to in the text

acquisitions were done by regular streaming and others via campaign measurements (see Table 1).

The backbone of IMO's operational geophysical monitoring network comprised of 25 cGNSS stations and 12 seismometers located within a 20 km radius of the eventual eruption site. The data were streaming in real-time (or NRT) to the operation monitoring room where the natural hazards specialists on duty 24/7 followed the evolution of the activity. In the pre- and syn-eruption phases, satellite products (Sentinel-1, CSK) were regularly acquired (with a frequency of between 1 and 8 days for CSK, and every 6 days for Sentinel-1 in both ascending and descending passes) to detect ground deformation signals. The ground-based and satellite-borne deformation observations and relocated seismicity were integrated via geodetic modelling and stress modelling to determine the location and source responsible for of the observed signals (e.g. for the dike intrusion, triggered seismicity and co-eruptive subsidence due to magma removal).

When the eruption started, the primary monitoring requirements were to observe the volcanic cloud and estimate its height and concentration of SO<sub>2</sub>, for assessing and forecasting the potential impact of volcanic gas pollution at ground level in populated areas. At the same time, tracking the lava flows and estimating effusion rate was needed to anticipate the probable evolution of the lava field and the local hazard affecting those visiting the eruption site. Ground-temperature probes, for continuous monitoring, were installed in cracks that had opened in the ground towards the northeast and southwest of the eruption site in the event that new fissures would continue to open endangering visitors.

DOAS (Differential Optical Absorption Spectrometer) is a UV remote sensing spectrometer that was used in both traverse and scanning modes to provide an estimate of SO<sub>2</sub> emitted at the source. A scanning DOAS was installed at about 10 km NNW of the

**Table 1** Overview of monitoring technique adopted in Iceland to follow the evolution of the eruption in Fagradalsfjall and the corresponding frequency of acquisition and type of data streaming

	Frequency of acquisition	Type of measurement and/or instrumentation
Streaming data	Continuous real-time or near-real-time (NRT)	Seismic network, Gas stations, Web cameras, Automatic Weather stations, Weather radars, Ceilometers, Lidars, Ground-temperature probes and Selected GNSS stations
	Several acquisitions per day	Cameras, Satellite products, MultiGAS and scanning DOAS, GNSS stations
	Several acquisition per week	Satellite synthetic aperture radar (SAR)
Campaign activity	Several acquisitions per week	DOAS traverses
	Sporadic collection	Tephra and rainwater collection, Drone-borne and ground-based MultiGAS, FTIR, Visual observations, Lava sampling and Surveillance flights for lava flow mapping

eventual eruption site prior to the eruption onset and two ready-to-be-deployed scanning systems were prepared so they could be quickly installed after the eruption started (Fig. 1; 6 km to the NW and 4.5 km to the SW). A DOAS system for making car and plane traverses was also prepared.

Ground-based and drone-borne MultiGAS measurements were made sporadically when possible. MultiGAS measures the composition of the volcanic gases H<sub>2</sub>O, CO<sub>2</sub>, SO<sub>2</sub>, H<sub>2</sub>S (and H<sub>2</sub> for some measurements) in situ (Pfeffer, et al., In preparation (2021a)). One MultiGAS was installed after the onset of the eruption close to the first vent, on a hill that was initially assessed to be “safe”, in relation to current lava flows (Fig. 2). Unfortunately for the station, the fifth fissure opened up very close to this site and subsequently destroyed it.

A network of passive gas samplers was installed around Fagradalsfjall to assess air quality close to the eruption site (Fig. 2). Two different types of systems were installed: Crowcon systems (Pfeffer et al., In preparation (2021a)) that measure SO<sub>2</sub>, H<sub>2</sub>S and CO<sub>2</sub>, and a bespoke system built using Alphasense sensors that measure SO<sub>2</sub>, O<sub>2</sub> and CO. Eventually, seven of these continuous gas monitoring systems were installed in a ring around the eruption site to account for variations in wind direction.

Prior to the eruption there was only one automated air quality monitoring station in the Reykjanes Peninsula measuring SO<sub>2</sub>. It was located in Grindavík and operated by the energy company HS Orka to monitor possible pollution from the Svartsengi power plant north of the town. About three weeks before the onset of the eruption, the Environment Agency of Iceland (EAI) began installing more automated monitoring stations. Five new SO<sub>2</sub> monitoring stations, with a resolution of a few µg/m<sup>3</sup>, were installed in the urban areas closest to the eruption site (Fig. 1). Shortly after the eruption began, six monitoring stations were running in municipalities closest to the eruption site, with a total exposed population of about 25 000 inhabitants. The distance from the eruption site to these stations in nearby villages was from 9 up to 18 km. Data from all these stations, as well as the near-eruption stations operated by IMO, were accessible on the open website [www.airquality.is](http://www.airquality.is).

There are over ten automatic weather stations on the Reykjanes Peninsula, and during the eruption one station was added close to the eruption site. These stations provided valuable real-time information on weather conditions and wind direction in the area, so people could plan a hiking route upwind from the main gas plume.

Since 2020, a ceilometer has been operating in Hvasshraun, 17 km NNE of the eruption site and a scanning lidar plus a ceilometer have been permanently located at Keflavík airport since 2015 (see Fig. 1). A mobile lidar was initially located in Reykjavík with the purpose of detecting potential volcanic aerosols dispersed towards or over the main capital area. However, on 1 July 2021 it was moved close to Grindavík to allow better coverage in the event the lava flowed to the sea. The fixed C-band weather radar at Keflavík airport 23 km to the NW, and a mobile X-band radar at Strandarheiði 13 km to the N, were also in operation, but due to the absence of volcanic ash in the atmosphere, their data was of limited use.

Visible and thermal cameras were installed in different places to allow both far-field and close views of the eruption site and eruptive activity (Figs. 1 and 2), several of which were already installed before the eruption started. Some of the cameras were calibrated to provide quantitative information on height of volcanic plumes and lava fountains (Barnie et al. 2021), evolution of the lava field through a front tracking processing, changes in the crater's geometries and the detection of active vents. Eventually, cameras were installed to provide a clear view of the areas where the lava field was advancing towards important localities like walking paths and valley ridges.



Tephra and rainwater collection buckets were deployed at different distances from the eruption site to assess the amount of fallen material and the level of pollution in the precipitation. The formation of pyroclasts was very minor and only occurred for a short period during the eruption.

The satellite thermal detection provided by MIROVA (Coppola et al. 2019, 2020) was regularly checked to monitor the level of activity and to keep track of the emission rates. Near real-time processing of Sentinel-5 products for SO<sub>2</sub> detection, provided a few images per day of long-range transport of the volcanic gas cloud and its magnitude.

Since the beginning of the eruption, photogrammetry of the lava field was acquired by aircraft. This information was vital for assessing the lava effusion rates, extent and emplacement style (Pedersen et al. 2021), as well as to initialize the lava flow simulations to anticipate the possible evolution of the lava field and potential area inundation.

## 4 Eruption chronology

The eruption commenced relatively quietly on the evening of 19 March at about 20:30 UTC (<https://en.vedur.is/about-imo/news/earthquake-swarm-in-reykjanes-Peninsula>) without any precursory escalation in either seismicity or deformation (Sigmundsson et al. 2022). The confirmation of its onset came from the people passing by the area and people from Grindavík, who phoned the IMO, as well as from the web cameras and satellite images. Lava initially erupted from a ~180 m long fissure which opened in a small valley, Geldingadalir in Fagradalsfjall (see Fig. 2) and that very quickly coalesced into two main adjacent craters (1a and 1b in Table 3). The lava started to pond in the valley and for almost two weeks no major changes affected the eruption scenario (Fig. 3).

Four main eruptive phases have been identified, as summarized in Table 2.

### 4.1 Phase I (19 March 2021–5 April 2021)

During the initial phase, the eruption progressed with a fairly stable extrusion rate, on average 4.9 m<sup>3</sup>/s (Pedersen et al. 2022), and 25–59 kg/s SO<sub>2</sub> was emitted (Pfeffer et al., in preparation (2021b)). Seismicity remained elevated during this period and about one thousand earthquakes >M1 (manually checked) were detected in the vicinity of the eruption site during the first two weeks.

### 4.2 Phase II (5 April 2021—27 April 2021)

Phase II of the eruption commenced on 5 April at 11:49 UTC (see Table 2) when two small new fissures opened about 600–800 m NE of the original eruption site (and merged into one vent in less than one day, 2ab in Table 3). This phase was characterized by the opening of additional fissures and lava extruding from these in variable amounts. Six additional fissures opened during the following eight days (Phase II-a in Table 2; craters 3, 4, 5abc and 6 in Table 3) all aligned along the orientation of the initial dike intrusion (Hjartardóttir et al., in preparation; Sigmundsson et al. 2022). On 14 April, amongst nine openings, seven were extruding lava, while gas and steam were being released at all active vents (see Table 2 and Fig. 4). During Phase II-b of the eruption the activity alternated between different craters, some of which stopped issuing lava, and others which became more powerful. There were no differences in the gas composition measured at the different vents but



**Fig. 3** **a** The large number of visitors formed a continuous line along the walking path to the eruption site. Photo taken on 24 March 2021; **b** People enjoying the view from the lower western slopes of Geldingadalir on 28 March 2021 (photos by B. Oddsson). In the months that followed both locations were covered with lava

there were different rates of  $\text{SO}_2$  emission measured along the active fissures. The timeline of the activity from the different craters active during Phase II-b is summarized in Fig. 4 and Table 3.

### 4.3 Phase III (27 April 2021 – 28 June 2021)

Web cameras show that after 27 April, lava production was coming from a single main vent (the fifth opening in temporal order, located at  $63.8906^\circ\text{N}$ ,  $22.2691^\circ\text{W}$ , 5b in Table 3)

**Table 2** The four main phases and corresponding sub-phases which characterized the eruptive activity in Fagradalsfjall, as described by different eruptive style and main associated hazards

	Time-period	Eruptive style	Main associated hazards
PHASE I	19 March 2021–5 April 2021	Effusive eruption from one main fissure	Gas pollution, lava flows
PHASE II	a 5 April 2021–14 April 2021	Effusive eruption from (up to) eight fissures + opening of new fissures	Gas pollution, lava flows, opening of new fissures, moss fires
	b 14 April 2021–27 April 2021	Effusive eruption from (up to) eight fissures	Gas pollution, lava flows, opening of new fissures, moss fires
PHASE III	a 27 April 2021–2 May 2021	Lava fountains from one main vent	Gas pollution, lava flows, opening of new fissures, moss fires
	b 2 May 2021–11 May 2021	Pulsating lava fountains from one main vent	Gas pollution, lava flows, opening of new fissures, bombs and tephra fallout
PHASE IV	c 11 May 2021–28 June 2021	Outpouring of lava from the main crater, with occasional lava fountains and persistent intra-crater activity	Gas pollution, lava flows, opening of new fissures
	a 28 June 2021–2 September 2021	Intermittent activity in the crater with long (few hours up to 4 days) intervals	Gas pollution, lava flows, opening of new fissures
	b 2 September 2021–18 September 2021	1-week-long repose followed 1-week-long activity	Sudden outbreak lava flows from upwelling area, gas pollution

**Table 3** The timing of the 9 openings that occurred in the first month of the eruption. In this scheme, the 2ab opening is considered one single crater given the very short-lived duration of the two initial openings. (\*)The crater 5b is the one which kept erupting throughout the entire duration of the eruption

Eruptive openings	Opening date	Opening time (UTC)	Duration of the activity	Coordinates (decimal degrees, EPSG:4326)
1a	2021-03-19	~20:30	Soon coalesced into 1b	63.8889, -22.2709
1b	2021-03-19	~20:30	~39 days	63.8892, -22.2706
2ab	2021-04-05	11:49	~12 days (the two openings coalesce into one source after ~1 day)	63.8952, -22.2637
3	2021-04-07	00:01	~20 days	63.8921, -22.2682
4	2021-04-10	03:13	~5 days	63.8934, -22.2662
5ab*c	2021-04-13	08:37 and 08:50	6 months	63.8910, -22.2689 63.8906, -22.2691 63.8905, -22.2685
6	2021-04-13	08:54	~15 days	63.8928, -22.2676

with variable lava outpouring (Phase III). Lava and gas were released through a fairly stable fountaining activity. Phase III-a lasted until 2 May, during which the lava fountains reached heights up to 120 m above the vent (about 350 m above sea level) (Fig. 5a). The activity then changed (Phase III-b) and was characterized by a very intense pulsating activity. At this point, lava fountaining occurred at regular intervals separated by a few minutes. Since this pulsating style commenced, the top height of fountains reached maximum levels of about 430 m above sea level (200 m above the vent), see Fig. 5a and 5b. Different gas compositions were measured by FTIR during and between lava fountaining events (Halldórsson et al. 2022; Pfeffer et al., in preparation (2021a)) and SO<sub>2</sub> concentrations directly above the vent were much higher during fountaining (Halldórsson et al. 2022; Pfeffer et al. in preparation (2021a)). The following phase (III-c) saw the alternation of lava fountains and intra-crater activity accompanied by sustained lava outpouring. The peak in lava fountains heights reached almost 500 m above sea level.

#### 4.4 Phase IV (28 June 2021–18 September 2021)

From 28 June until the 18 September (Phase IV) the activity became less sustained and was characterized by pauses in activity in the crater for several hours (up to 35 h consecutively in Phase IV-a and one week in Phase IV-b). During the pauses in activity, the SO<sub>2</sub> flux dropped to relatively low levels. In Phase IV-b the lava originated from an upwelling region (~500 m SW of the main crater) which fed fast flows which were difficult to anticipate and to reproduce by numerical models. Since 18 September no surficial activity was detected and no new lava emitted from this crater.

Throughout the 2021 eruption and the different phases, a thick and dense gas-rich plume was often visible which rose up to several kilometres due to buoyancy and inertial momentum (Fig. 6b). A time series overview of plume top and bottom height as measured from Hvassahraun camera (~12 km NE of the eruption site) is provided in Fig. 6a and shows a plume extending between a few hundred metres and 3000 m asl in the first month of the eruption. The month of May was characterized by an increasing

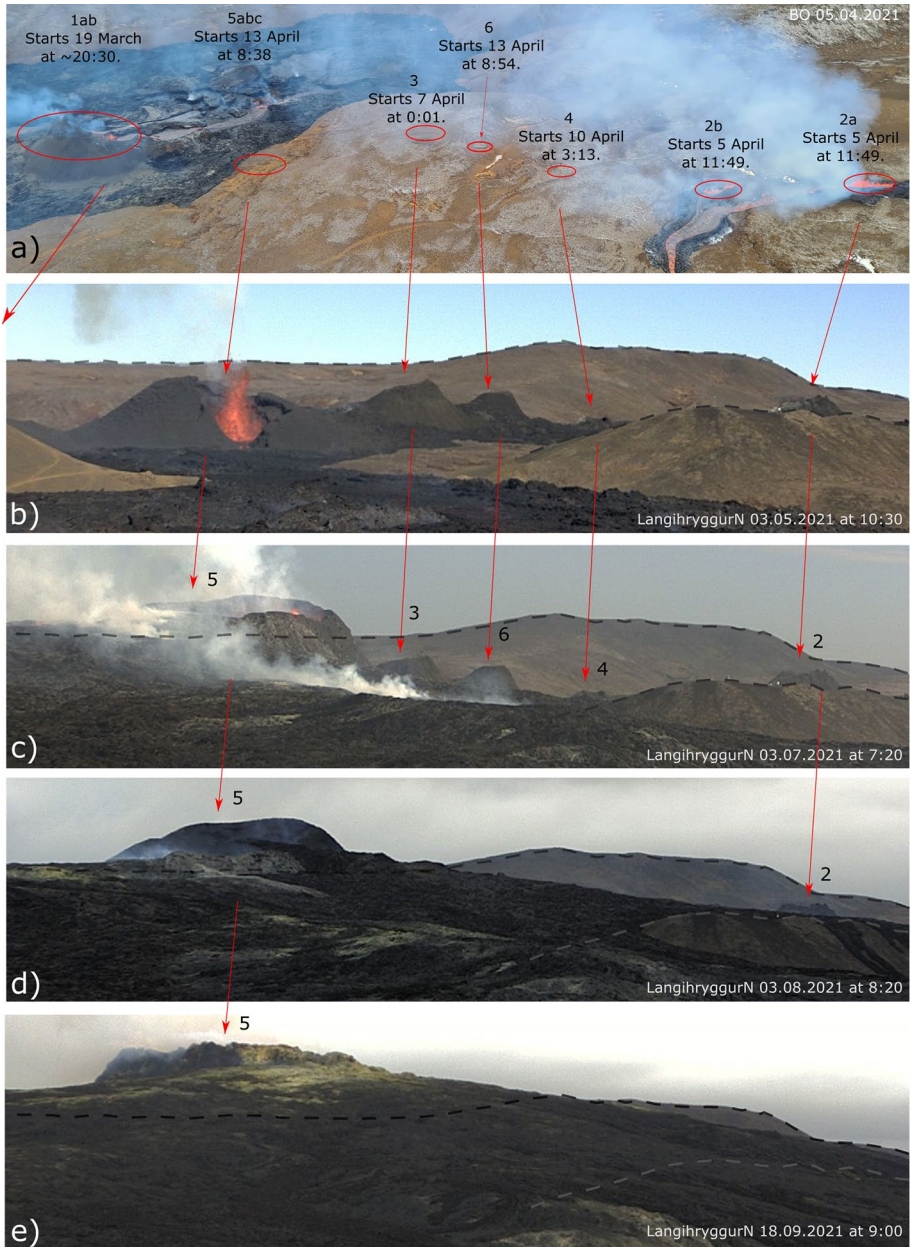


**Fig. 4** **a** Locations of eruptive openings and their timing, superimposed on a photo taken from the air on 5 April 2021; Evolution of the main crater (N. 5) **b** 03 May, **c** 03 July, **d** 3 August and **e** 18 September. Photos from a webcam located on Langihryggur, 1.4 km to the southeast of the main crater (Fig. 2—green arrow). Note how the increasing height of the lava gradually obscures the view to the openings active in April

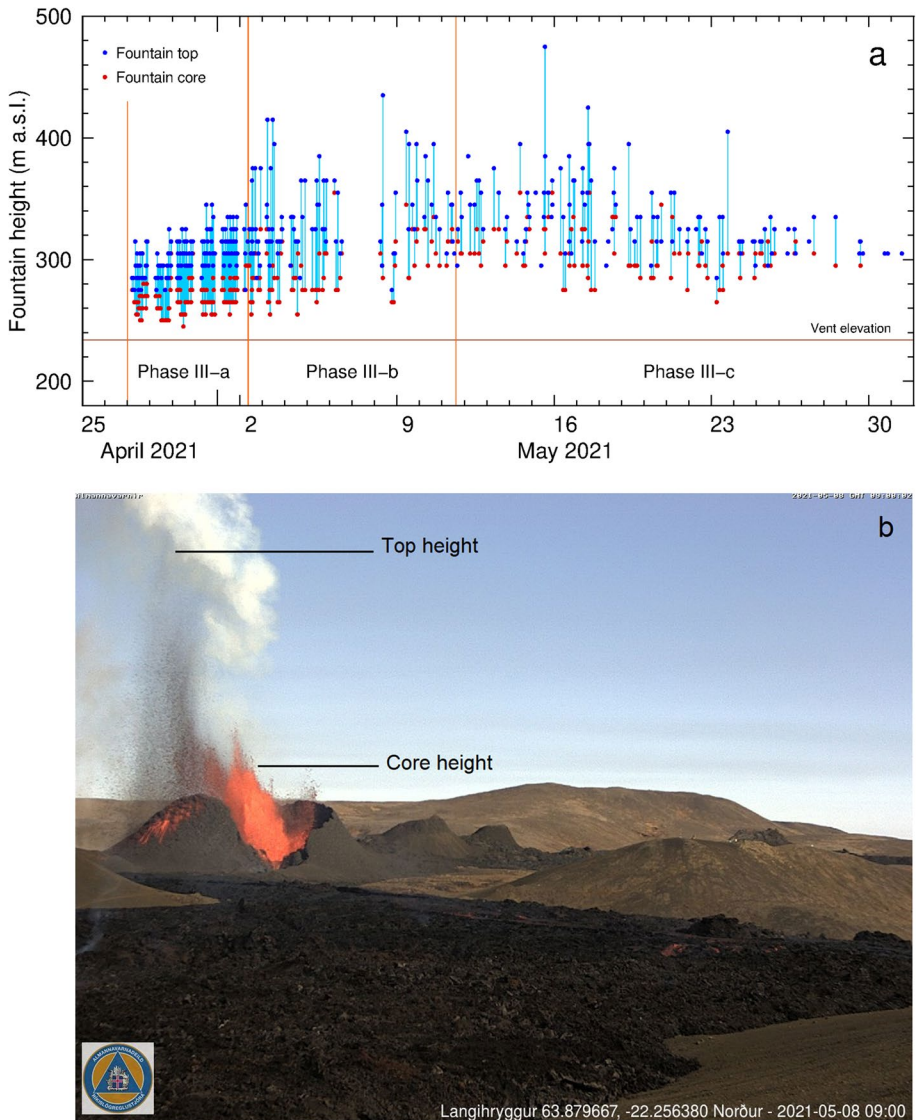


**Fig. 5** **a** Temporal evolution of lava fountain height as seen from the camera in Langihryggur (Fig. 2—green arrow) for the period 27 April - 31 May 2021. The top height is defined by the highest point reached by pyroclasts, whereas the core height is defined as the height reached by continuous fountain. Both heights are measured using a calibration of the images and the known horizontal distance between vent and camera; **b** example of lava fountain on 8 May 2021 as seen from Langihryggur camera

plume height which ascended to 4100 m asl. This increase coincided with a change in meteorological conditions characterized by a stable atmosphere, with low wind speed ( $< 10$  m/s) that persisted throughout a three-week-long period. The plume top height eventually decreased again staying below 2000 m for most of June and part of July. Around mid-August plume top heights again reached up to 3000 m asl. No good

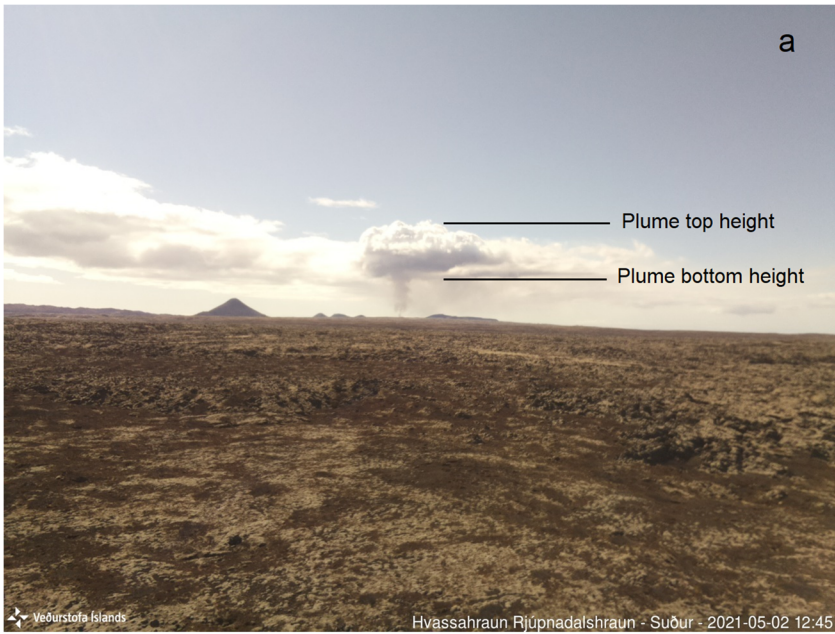
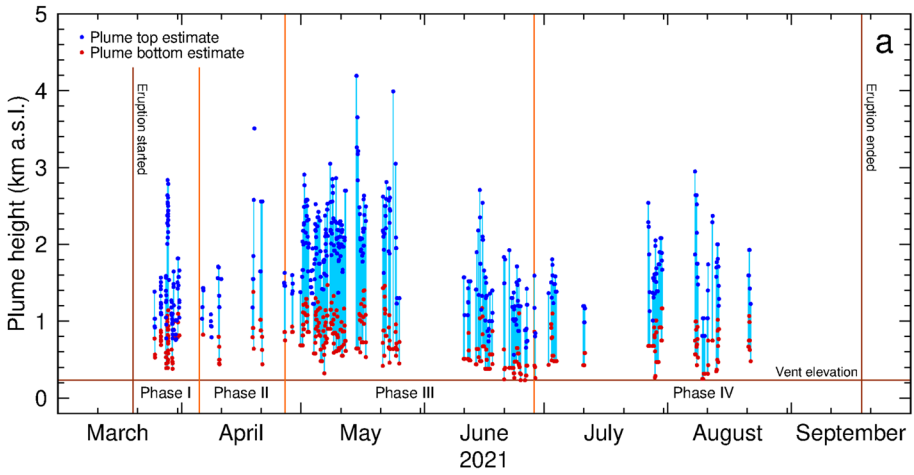


**Fig. 6** **a** The plume height as function of time as observed from the Hvasshraun camera for the period 25 March–21 August 2021; **b** The volcanic plume from Fagradalsfjall eruption on 2 May 2021 as seen from the Hvasshraun camera (see Fig. 1—green circle)

observations of the plume were acquired in September. For many weeks after the eruption ended, the rising heat from the lava field created a clear plume during favourable meteorological conditions.

## 5 The associated hazards

The vicinity to populated areas as well as to the Keflavík international airport facilitated access for a large number of visitors to the eruption site from the first day of the eruption. Up to 6000 people per day visited the eruption site at the beginning of the eruption (Icelandic Tourism Dashboard 2022), often forming crowded queues along the main walking paths and many staying in the vicinity of the lava field until evening waiting to take night-time photos (Fig. 3a and b). They walked along a faintly marked path into the area, which initially was without any sort of infrastructure, such as parking lots, secure paths or information signs. This presented a challenge for both the local rescue teams and the police who managed access to the area, as well as for Civil Protection who was in charge of the risk evaluation (<https://www.almannavarnir.is/english/general-information/emergency-response/> and Barsotti et al. 2020a, 2020b). Initially, access was allowed in most areas around the eruption site, however, with the progression of the events, changes were implemented to define a hazard zone where people were advised not to enter. The main hazards considered were the opening of new eruptive fissures, lava flows, gas pollution, spatter and tephra fall, and, to a lesser extent, dissolved constituents in precipitation.

### 5.1 Opening of new fissures

On 5 April the second eruptive fissure opened (also in a very silent manner) with no apparent precursors observed by the monitoring network. The new opening was first observed by people visiting the eruption who watched it happening. This second opening occurred about 600–800 m NE of the active crater and aligned along the main NE-SW direction of the mapped pre-eruptive dyke intrusion. Additional openings occurred on 7, 10 and 13 April, and they were all located between the first two main fissures (see Fig. 3, Table 2). The seismic monitoring revealed that on many occasions, the tremor, as detected by several stations near the eruption site, showed a sharp decrease in intensity (2–4 Hz band) prior to the opening of new fissures (Soubestre et al., in preparation). Even though it triggered occasional false positives, this was subsequently used as one of the criteria to alert the Civil Protection and those operating in the area to the potential of new openings. The possibility of an eruptive opening with no warning was considered the highest risk for those visiting the area (both tourists, monitoring staff and scientists). This led to the installation of the continuous ground-temperature instruments to possibly provide some warning prior to new crack openings. In addition, the implementation of real-time processing of cGNSS data from stations closest to the active area was set up to anticipate the occurrence of new openings.

### 5.2 Lava flows

The eruption between the 19 March and 18 September was effusive, and as such lava flows were one of the main eruptive hazards. The area where the eruption took place is far from inhabited regions and no major infrastructure was directly exposed to lava inundation. Through regular aerial monitoring surveys and photogrammetry, it was possible to track lava field evolution and to assess the extrusion rate. The last survey confirmed that a total of  $150 \pm 3 \times 10^6$  m<sup>3</sup> bulk volume of lava had been extruded over a six-month period and the emplaced lava field covered an area of 4.8 km<sup>2</sup> (Pedersen et al.



2022). Lava flows were issued from all fissures/openings, so that the lava propagated both towards the NE (Meradalir valley after 5 April) and towards the SE (Syðri-Meradalur valley after 14 April) after ponding for the first four weeks in the Geldingadalir valley. On 22 May the lava also started to flow down the Nátthagi valley through Syðri-Meradalur and on 13 June lava spilled from Geldingadalir over hiking trail A into Nátthagi, raising concern that lava might flow towards the south-coast road and eventually enter the sea (see Fig. 2).

Cameras installed close to the eruption site (owned by IMO, the Icelandic Civil Protection and two TV channels) enabled the tracking of the lava fronts in different directions (see Fig. 2). The lava flow propagation was modelled using the MrLavaLoba numerical code (de' Michieli Vitturi and Tarquini, 2018; Tarquini et al. 2018) to anticipate the areas that might be inundated by lava, the most likely transport direction of active lava fronts and the potential timing of the filling of valleys and resulting spill over events. New fissures opening, coupled with variations in lava transport mechanisms, made it challenging to successfully reproduce recent and current flow activity with model simulations.

### 5.3 Gas pollution

The gas stations installed in communities and near the eruption site were essential to be able to advise communities about gas pollution. Following the experience gained during the Bárðarbunga eruption (Gíslason et al. 2015; Pfeffer et al. 2018), station installation, data streaming, and communication and assessing potential pollution hazards from the eruption was relatively straightforward. A reference table correlating hazardous SO<sub>2</sub> concentration limits and suggested actions to take in case of exposure to such pollution was used, as during the eruption in 2014–2015 (<https://ust.is/english/air-climate/air-pollution-during-a-volcanic-eruption/>). Throughout the eruption, very few community stations in the Reykjanes Peninsula detected high levels of SO<sub>2</sub>, with the highest concentrations recorded in Njarðvík on 7 April (Fig. 7a). On that occasion the 10-min concentration in air was up to 2000 µg/m<sup>3</sup> (Whitty et al., in preparation). The measurements at ground level were used for both warning people and to validate the forecast model. The stations in the vicinity of the eruption site, operated by IMO (see Fig. 2), were used to alert workers and visitors about dangerous levels of pollution in the area (Fig. 7b). The concentration of SO<sub>2</sub> often reached critical conditions near the eruption site, well beyond the documented safe levels established by the Environmental Agency of Iceland (EAI). The high concentrations varied both spatially and temporally and it was always possible for people to move away from the dense gas region to areas with safer concentrations.

In addition to the fresh plume transported directly from the eruption site to target areas, several cases of pollution due to a mature plume, richer in the oxidized sulphur species sulphate, were detected. These events were interpreted to be an evolved eruption cloud where the SO<sub>2</sub> converted into particulates of SO<sub>4</sub><sup>2-</sup> in the atmosphere (Carlsen et al. 2021; Ilyinskaya et al. 2017). An example is shown in Fig. 8 where the temporal evolution of SO<sub>2</sub>, PM<sub>2.5</sub> and PM<sub>1</sub> concentrations are all plotted together for a station in Reykjavík (Bústaðavegur), 37 km NE of the eruption site, for the period 28 June–7 July. The simultaneous presence of elevated concentration of fine particles (PM) and SO<sub>2</sub>, detected on 2–3 July, indicates the presence of a mature volcanic cloud.

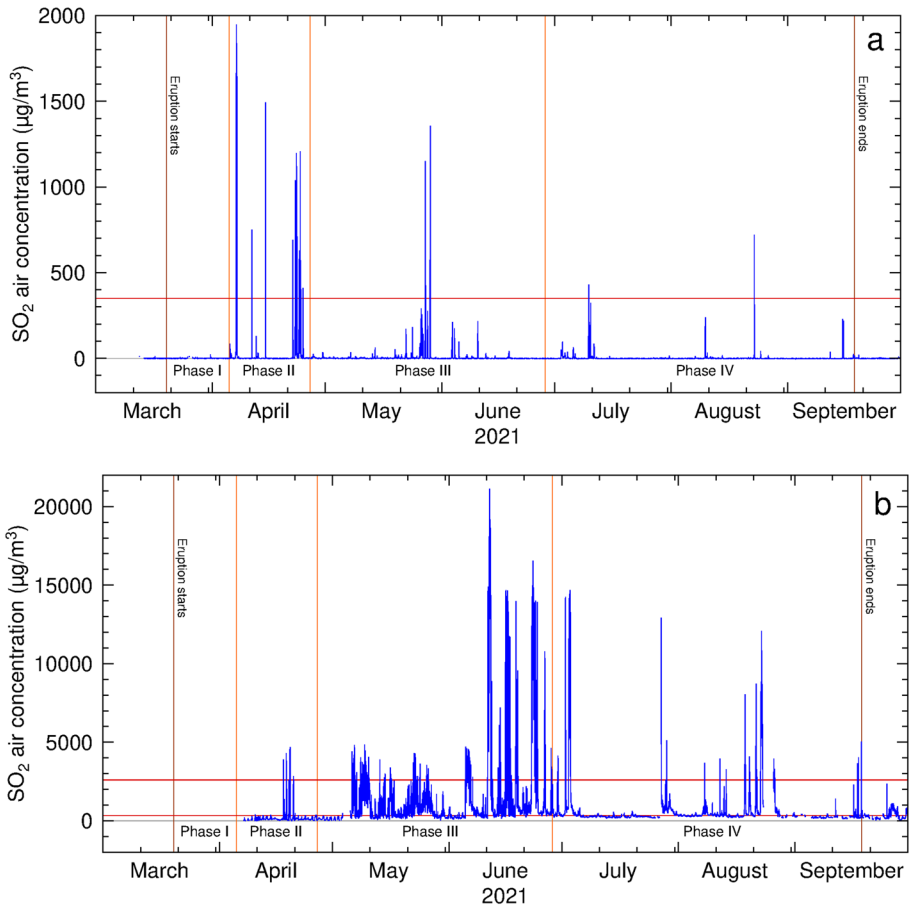


**Fig. 7** **a** Temporal evolution of 10-min SO<sub>2</sub> concentration at the station in Njarðvík (about 14 km NW of the eruption site—purple circle in Fig. 2); **b** the SO<sub>2</sub> temporal evolution at one of the stations in closer proximity to the eruption site (about 550 m South of the main crater—brown arrow in Fig. 2). Both plots show the concentration for the entire eruption period. The two red horizontal line refers to the limit of 350 (thin) and 2600 (thick) µg/m<sup>3</sup> as established by the Environmental Agency of Iceland for the first levels of pollution of concern for humans

## 5.4 Spatter and tephra fall

Fresh lapilli fell in the area surrounding the eruption site (Fig. 9). A survey undertaken during the first two weeks of the eruption showed mm-sized pumices that landed up to 600 m from the active vent with occasional cm-sized clasts observed. Pele's hair up to tens of cm were observed up to 2 km away from the vent. Initially the hazard impact due to the fallout of this material was assessed to be quite localized, but this changed when the activity became pulsatory at the beginning of May (see Table 2).

In May, the intense fountaining and the ensuing greater heights reached by pyroclasts allowed the material to land further away from the main crater. 10-cm sized and larger spatter were identified initially at a distance of 500 m from the crater and subsequently up to 1.5 km. Occasional strong winds facilitated the transport of very light and wide spatter

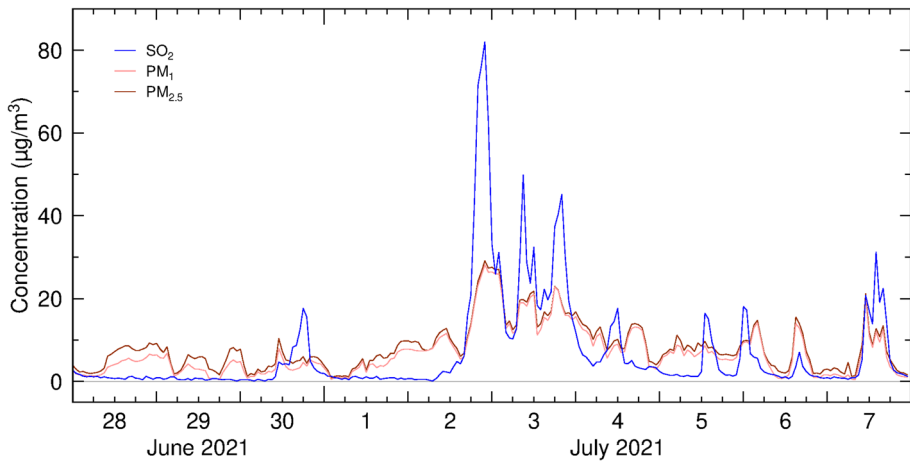


**Fig. 8** Temporal evolution of  $\text{SO}_2$  and PM (2.5 and 1) at the Bústaðavegur station in Reykjavík (Fig. 1 for location) for the period 28 June–7 July showing the temporal correlation between the different species which confirms the presence of volcanic sulphate in the plume reaching the Capital area

of lava up to a distance of 1.7 km, and it was not uncommon to be showered by lapilli rain if downwind of the eruption site. The hot spatter landing in dry moss sometimes caused short-lived fires. In the light of this new hazard, collection buckets were set out around the eruption site for periodic collection, with the main aim of collecting tephra samples at different distances and to allow for proper assessment of pyroclast fallout and the implication for people on site.

## 5.5 Dissolved constituents in precipitation

More than 320 samples of precipitation were collected from 12 stations around the eruption, some close to the eruption site and some in the closest urban areas (Figs. 1 and 2). Twenty-nine samples were additionally taken from five lakes on the Reykjanes Peninsula. Chemical analysis of the precipitation and lake samples was used to estimate the potential impact on the environment, animal health and groundwater in the vicinity of the eruption (~7.5 km). Analyses were made for pH and 48 elements (including F, Cl,  $\text{SO}_4$ , Si, Mg).

Prior the eruption (or at its very beginning), pH in precipitation was measured in Keflavík (less than 20 km from the eruption site) and in Reykjavík (less than 50 km). In areas with scarce vegetation and young lava, as most of Iceland, the alkaline impact of dust on the precipitation composition can be quite high (Gíslason et al. 2015) and this explains the high pH values measured in Keflavík (7.2) and Reykjavík (5.9). However, since the beginning of the eruption, pH measured at the eruption site was constantly very low, on average 3.51, with the lowest measurement of 2.64. Concentration of all measured elements was elevated in most of the samples with the highest concentrations at the eruption site and at sites to the north of the eruption (see Fig. 1). Extremely high concentration peaks were measured in precipitation in two periods: late March (23–25 March) and early April (31 March–05 April). In the first week of April, F concentration of 219.5 ppm was measured at the eruption site compared to 0.81 ppm in the lowest measured sample at this site (18 May). The second highest concentration (83.5 ppm) was measured in the same location in late March. The average of all the samples for the summer period was about 14 ppm F,



**Fig. 9** Pumice clasts produced during the Fagradalsfjall eruption. **a** Pumice clasts (green arrows) on the valley slopes about 600 m NNW of the Geldingadalir craters, produced during phase I of the eruption, as seen on 24 March 2021. **b** Pumice clasts collected on 24 March 2021 from the general area shown in (a). The long axes of clasts are up to 2.8 cm, although most grains are <1 cm in diameter (see a). **c** Pumice clasts (green arrows) in Nátthagi, about 2.5 km SSW of active vent, produced in May 2021 during phase V of the eruption, as seen on 19 May 2021. **d** Pumice clasts collected on 19 May 2021 from the general area shown in (b). The long axes of clasts are up to 6.2 cm. Photos: Bergrún Arna Óladóttir

with an expected typical level of  $\sim 0.02$  ppm that was measured repeatedly throughout the eruption period. The other elements listed above show similar patterns.

## 6 Discussion

### 6.1 Fagradalsfjall volcanic eruption as a tourist attraction

The eruption at Fagradalsfjall emitted a total amount of  $\text{SO}_2$  equal to  $967 \pm 538$  kt 9 (Pfeffer et al. in preparation (2021b)) and a total bulk volume of lava of  $0.150 \pm 0.003$   $\text{km}^3$  (Pedersen et al. 2022). This indicates that the Fagradalsfjall 2021 eruption was of approximately average size for Iceland (Gudmundsson et al. 2008). However, it was small compared with the most recent basaltic eruption in Iceland, within the Bárðarbunga volcanic system in 2014–2015, when 9.2 Mt of  $\text{SO}_2$  was released and  $1.4$   $\text{km}^3$  of lava was extruded (Pedersen et al. 2017; Pfeffer et al. 2018) during a similar 6-month long eruptive period. However, the Fagradalsfjall eruption was distinctively hazardous, given its vicinity

to inhabited areas and critical infrastructure, as well as the high number of visitors to the site, representing new challenges for both scientists and civil protection representatives. Its location between the International Airport of Keflavík and the Reykjavík Capital area, facilitated the access of numerous visitors to the eruption site. Holuhraun, in contrast, was an extremely remote location and access to the site was restricted during the 2014–2015 Bárðarbunga eruption. The Fagradalsfjall eruption therefore provides an excellent case study of a popular “touristic” eruption, which both individuals and organized tour groups came to visit. The former for experiencing the forces of nature, the latter for obvious economic interests (Donovan 2018).

Based on the data from the Icelandic Tourist Board (2022) about 356,000 people visited the eruption site during the period 24 March 2021–7 January 2022. During the first month of the eruption the number of visitors per day reached 6000 and comprised mostly local tourists. From June 2021, in correspondence to the border opening (following the COVID restriction release by the government), the tourism became more international. Despite the high number of visitors to the area, rough hiking trails and elevated SO<sub>2</sub> levels, there were no fatalities.

Eruptions with high tourist interest require ongoing monitoring and relevant and timely information delivered to authorities to inform decision-making and evolving mitigation actions. Throughout the eruption, the goal was to provide a low risk access route to the site, established and reviewed via regular and frequent (initially daily) meetings between the IMO’s surveillance room and its managers, selected scientists, Civil Protection representatives, police and rangers from the environmental institute that patrolled the area on a daily basis. The latest observations, forecasts, and hazard assessment were communicated and discussed. Those attending the meeting had the chance to look at the scientific data and consider the implications for their actions in the field, like rerouting the walking paths, diverting people to more secure areas, and temporarily closing the area due to bad weather or expected high concentration of gas at ground level.

## 6.2 Responding to the volcanic hazards

Throughout the duration of the eruption, the types of associated hazards were changing along with variations in the eruptive style, reflecting a dynamic eruption requiring a dynamic response. The hazards included: air pollution (both SO<sub>2</sub> and sulphates), acid precipitation, water and ground pollution, electrification of air, and, on a more local scale, ground fracturing, opening of new eruptive fissures, lava flows and lava spill over, tephra fallout and moss fires. Throughout the evolution of the eruption, the hazard assessment was also changing and needed to be adaptable to account for additional volcanic phenomena. However, different volcanic hazards had different temporal and spatial scales and for this reason different approaches were used for dealing with a local assessment, constrained to the eruption site, and a proximal zone (within 50 km). No direct hazards were identified that posed a significant threat to the far-field, even though an occasional increase in SO<sub>2</sub> concentration was detected as far as Akureyri on 25 June (~280 km NE of the eruption site). In addition to the Reykjavík Capital area, where about 237,000 people live (Statistics in Iceland 2022), there are several inhabited centres within a distance of 50 km from Fagradalsfjall: Keflavík and Njarðvík (19,600), Grindavík (3500), Sandgerði (1900), Garður (1700), Vogar (1300) and Hafnir (100). In all, over 264,000 people (72% of Iceland’s population) lived near the eruption site and were directly exposed to primary volcanic hazards.

As soon as the eruption started a forecasting system was implemented at the IMO with the purpose of informing people living on the Peninsula about the anticipated danger due to volcanic pollution. The CALPUFF dispersal code was reinstated (used during the Holuhraun eruption) to reproduce the SO<sub>2</sub> emission and transport from Fagradalsfjall (Barsotti et al. 2020a, 2020b; Scire et al. 2000). The 48-h forecast of ground concentration of SO<sub>2</sub> was available on IMO's website. The hourly forecast was shown using the colour system used by the EAI (Directorate of Health 2021) which follows the reference SO<sub>2</sub> thresholds. There was a public expectation of frequent, very detailed, precise, and accurate forecasts. However, this was impractical to generate in a timely matter given available models, data, and computation resources. Instead, we provided two additional maps that indicated the most likely location and timing of impacted (ground level) areas within the next 6 and 24 h. These additional maps did not convey the intensity (severity) of pollution during the indicated timeframe (Barsotti 2020a, 2020b). People were asked to check on the EAI website for the real-time measurement at the closest municipal station whenever the plume was forecasted to be near to them.

On a more local scale, the hazard assessment focused on dynamic phenomena that would have the potential to threaten people visiting the eruption site. The possibility of sudden fissure openings, high levels of volcanic gas, advancing lava fronts and lava outbreaks towards hiking trails, and occasional tephra fallout, all needed to be considered to ensure low risk access. When the first “dangerous area” map was designed, the aim was to identify the area where additional openings were more likely to occur, based on the proximity to the modelled dyke intrusion at depth. This area was considered a high-danger region and people advised not to enter it. Subsequent hazard maps accounted for the extension of the lava field (as reconstructed mainly via aerial photogrammetry) by adding an extra buffer zone of about 100 m and was intended to prevent people from being subject to sudden lava outbreaks and exposure to fluid lava and high temperatures. The lava flow modelling results were not included into such maps as their temporal uncertainty was too large and the maps would have been prone to public misunderstanding. The on-line ballistic trajectory tool developed by Mastin (2001) was adopted to identify preliminary contours of the hazard area effected by volcanic clasts fallout. Both calm and high-wind conditions were considered, as the wind in the Fagradalsfjall area could reach very high speeds (through the eruption duration the strongest measured wind was 34 m/s on the 12 May, with wind gusts up to 48 m/s). The density of individual pyroclasts were very low (roughly 500 g/m<sup>3</sup>) that the presence of wind led to a greater transport distance. Two circles of 500 m and 650 m radii were eventually added to the map, identifying the area where people were advised that in given conditions such fallout might occur (see Fig. 10). This area was primarily used by the air-traffic controller for helicopters to advise on where they might land when bringing people to the eruption site. The hazard map (Fig. 10) was formally published on-line by the Icelandic Meteorological Office on 4 May 2021 and endorsed by the Civil Protection which passed it on through key dissemination channels like Safe Travel (safetravel.is).

As the forecast of gas pollution over such a small area would have required a very precise numerical model and high-resolution meteorological data that were not available, the decision was taken to not attempt to model it. Rather, we informed people that pollution due to volcanic gas was expected anywhere surrounding the eruption site. Visitors were asked to check the daily written forecast prepared by the weather forecaster on-duty, available on IMO's website, as well as directing them to the real-time data streaming from the stations installed at the eruption site which was available on EAI's website. In the first weeks of the eruption, when the rescue team volunteers detected elevated gas concentrations with their hand-held sensors, they would instruct people to leave the area and move

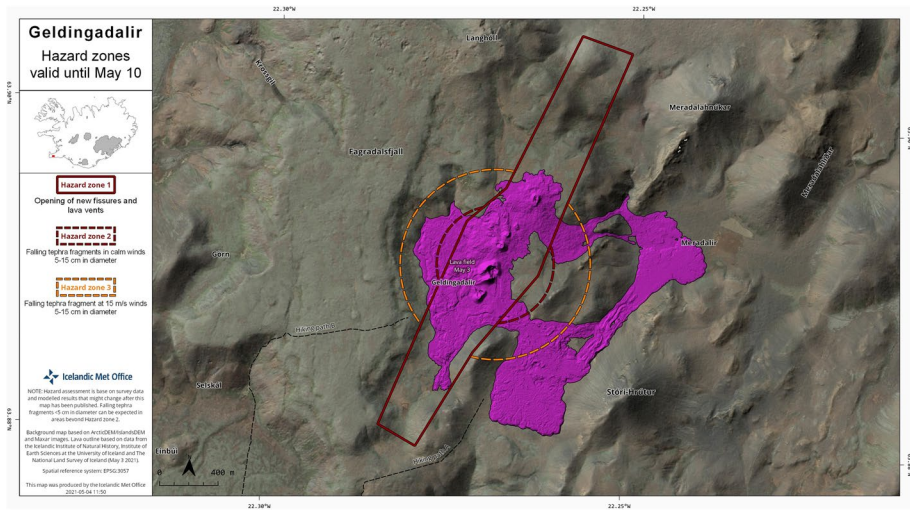


**Fig. 10** Hazard map prepared in May 2021 indicating the area where new fissure openings were considered possible (red polygon) and area where fallout of large clasts from lava fountaining could happen (orange and red circles). The extent of the lava field at the time of making was also reported for reference. The map was adopted by Civil Protection and local Police for controlling and managing accesses to the eruption site

upwind and to elevated places to avoid direct exposure. CP advised visitors to not bring babies or pets to the eruption site. The level of pollution of surficial water was regularly reported to civil protection and recommendations were given to discourage to bring dogs or horses who might drink polluted water puddles.

Mitigation actions and coordinated response, as those listed above, ensured that most visitors were able to experience the volcanic activity from low risk locations. However, it is also important to mention those occasions when support and intervention was required by local rescue teams. This included search and rescue for people lost during bad weather (mainly in the beginning of the eruption). Five people in total needed to be rescued by helicopter, three because of injuries along the walking path and two as they remained trapped by lava flows; more than 30 people asked for assistance due to exhaustion and/or hypothermia, and possibly gas poisoning (up to 30 people sought medical attention at the Poison centre at the hospital for examinations); 25 people suffered fractures and more than 30 needed assistance for other types of injuries (Landsbjörg, personal communication).

### 6.3 A new potential scenario

As lava flow entered Náttagi, the reality of no natural obstacles between the flow and the ocean 1.5 km away prompted considering the possibility of lava entering the ocean. While this unusual scenario did not eventuate, preparations involved running the MrLavaLoba model to produce a short-term forecast and identify the most likely ocean entry point (Fig. 11).

In Iceland, lava flows last entered the sea during the Heimaey eruption in 1973. This would trigger additional hazards to take into consideration. Amongst others the most relevant hazards considered were:





## 7 Conclusion

At the time of writing (November 2022), eruptive activity at Fagradalsfjall has ceased, but the entire Peninsula is still characterized by persistent seismicity. The future of this unrest is currently difficult to foresee but may comprise multiple additional dike intrusions over the coming years, which may or may not culminate in eruptions. The activity at Fagradalsfjall has proven to be an invaluable opportunity to investigate and learn more about pre-eruptive monitoring, data interpretation, fissure eruption dynamics, low-level volcanic gases dispersal processes, lava flow simulation, volcanic hazard assessment and communication.

Its location and its easy access made this eruption very touristic with more than 356,000 visitors since March 2021 (considering only the first eruption in 2021). Managing the accessibility to the site required strong collaboration between scientists and civil protection authorities. It has always been an Icelandic cultural priority that natural phenomena, even when potentially dangerous, should be safely enjoyed by people. Regular meetings between scientists and those in charge of operations, sharing of scientific data and numerical model results and an open dialogue have been essential ingredients for managing health and safety issues deeply related to volcano tourism.

This paper also reveals how important it is to define scenarios (based on monitoring data and/or numerical model results) for advanced preparation of monitoring setup, monitoring strategies and identification of hazards.

**Author's contribution** SB and MMP conceived the paper and wrote the manuscript; MAP, BAÓ, TB, MMT, KJ, GBMP, ÁRH, GS, TJ, TH, SvL, GNP, EMS contributed in collecting data, provided the data analysis and contributed to the text; ÞA, RHP took care of the graphics, plotting data and contributed to the text; MTG contributed in reviewing the text and images; BO, BGÓ, KV and HG were essential part in managing the crises and bringing input to the analysis provided in this manuscript.

**Funding** This paper represents independent research part-funded by the International Civil Aviation Organization (ICAO) through the Joint Finance Agreement.

**Data availability** Most of the monitoring data from the Icelandic Meteorological Office are available at the IMO's website: <https://en.vedur.is/>. Specifically, the earthquakes list is available and downloadable at the page <https://skjalftalisa.vedur.is/#/page/map>. Most of the news regarding the Fagradalsfjall eruption are still accessible at the link: <https://en.vedur.is/volcanoes/fagradalsfjall-eruption/news-and-alerts/>. Data from air quality stations in Iceland are accessible and downloadable at the Environment Agency of Iceland website at the link: <https://loftgaedi.is/en?zoomLevel=7&lat=64.894972&lng=-18.675028>. Plume height time series, reconstructed by using calibrated cameras, is available upon request to the authors.

## Declarations

**Conflict of interest** The author(s) declare no competing interests.

**Open Access** This article is licensed under a Creative Commons Attribution 4.0 International License, which permits use, sharing, adaptation, distribution and reproduction in any medium or format, as long as you give appropriate credit to the original author(s) and the source, provide a link to the Creative Commons licence, and indicate if changes were made. The images or other third party material in this article are included in the article's Creative Commons licence, unless indicated otherwise in a credit line to the material. If material is not included in the article's Creative Commons licence and your intended use is not permitted by statutory regulation or exceeds the permitted use, you will need to obtain permission directly from the copyright holder. To view a copy of this licence, visit <http://creativecommons.org/licenses/by/4.0/>.

## References

















- Árnadóttir T, Lund B, Jiang W, Geirsson H, Björnsson H, Einarsson P, Sigurdsson T (2009) Glacial rebound and plate spreading: results from the first countrywide GPS observations in Iceland. *Geophys J Int* 177(2):691–716
- Barnie T, Sigurðsson T, Pfeffer MA, Arason P, Barsotti S (2021) A calibrated visual web camera network for measuring volcanic plume heights: technical aspects and implementation for operational use. *Eur Geophys Union*. <https://doi.org/10.5194/egusphere-egu21-15235>
- Barsotti S (2020) Probabilistic hazard maps for operational use: the case of SO<sub>2</sub> air pollution during the Holuhraun eruption (Bárðarbunga, Iceland) in 2014–2015. *Bull Volcanol* 82(7):7
- Barsotti S, Oddsson B, Gudmundsson MT, Pfeffer MA, Parks MM, Ófeigsson BG, Sigmundsson F, Reynisson V, Jónsdóttir K, Roberts MJ, Heiðarsson EP, Jónasdóttir EB, Einarsson P, Jóhannsson T, Gylfason ÁG, Vogfjörð K (2020) Operational response and hazards assessment during the 2014–2015 volcanic crisis at Bárðarbunga volcano and associated eruption at Holuhraun, Iceland. *J Volcanol Geotherm Res* 390:106753. <https://doi.org/10.1016/j.jvolgeores.2019.106753>
- Björnsson S, Einarsson P, Tulinius H, Hjartardóttir ÁR (2020) Seismicity of the Reykjanes Peninsula 1971–1976. *J Volcanol Geoth Res* 391:106369
- Brander JL, Mason RG, Calvert RW (1976) Precise distance measurements in Iceland. *Tectonophysics* 31(3–4):193–206
- Carlsen HK, Ilyinskaya E, Baxter PJ, Schmidt A, Thorsteinsson T, Pfeffer MA, Barsotti S, Dominici F, Finnbjörnsdóttir RG, Jóhannsson T (2021) Increased respiratory morbidity associated with exposure to a mature volcanic plume from a large Icelandic fissure eruption. *Nat Commun* 12(1):1–12
- Clifton AE, Kattenhorn SA (2006) Structural architecture of a highly oblique divergent plate boundary segment. *Tectonophysics* 419(1–4):27–40
- Coppola D, Barsotti S, Cigolini C, Laiolo M, Pfeffer M, Ripepe M (2019) Monitoring the time-averaged discharge rates, volumes and emplacement style of large lava flows by using MIROVA system: the case of the 2014–2015 eruption at Holuhraun (Iceland). *Ann Geophys* 61:52
- Coppola D, Laiolo M, Cigolini C, Massimetti F, Delle Donne D, Ripepe M, Arias H, Barsotti S, Parra CB, Centeno RG (2020) Thermal remote sensing for global volcano monitoring: experiences from the MIROVA system. *Front Earth Sci* 7:362
- Cubuk-Sabuncu Y, Jónsdóttir K, Caudron C, Lecocq T, Parks MM, Geirsson H, Mordret A (2021) Temporal seismic velocity changes during the 2020 rapid inflation at Mt. Þorbjörn-Svartsengi, Iceland, using seismic ambient noise. *Geophys Res Lett* 48(11):e2020GL092265
- de’Michieli Vitturi M, Tarquini S (2018) MrLavaLoba: a new probabilistic model for the simulation of lava flows as a settling process. *J Volcanol Geotherm Res* 349:323–334
- Directorate of Health (2021) Health Risks due to air pollution from volcanic eruptions—Guidelines for the public. [https://www.landlaeknir.is/servlet/file/store93/item45005/Haetta%20a%20heilsutjoni%20vegna%20loftmengunar\\_EN%202.pdf](https://www.landlaeknir.is/servlet/file/store93/item45005/Haetta%20a%20heilsutjoni%20vegna%20loftmengunar_EN%202.pdf)
- Donovan A (2018) Sublime encounters: commodifying the experience of the geos. *Geo Geogr Environ* 5(2):e00067
- Einarsson P (1991) Earthquakes and present-day tectonism in Iceland. *Tectonophysics* 189(1–4):261–279
- Einarsson P (2008) Plate boundaries, rifts and transforms in Iceland. *Jökull* 58(12):35–58
- Einarsson S (2019) Krýsuvík. In: Óladóttir B, Larsen G, Guðmundsson MT (eds) *Catalogue of Icelandic Volcanoes*. IMO, UI and CPD-NCIP. Accessed from <http://icelandicvolcanoes.is/?volcano=KRY>
- Foulger G, Bilham R, Morgan WJ, Einarsson P (1987) The Iceland GPS geodetic field campaign 1986. *EOS Trans Am Geophys Union* 68(52):1809–1818
- Gaudru H (2014) *Volcano tourism: the effect of eruptions and disasters*. Volcanic tourist destinations. Springer, Berlin, pp 337–350
- Geirsson H, Árnadóttir T, Hreinsdóttir S, Decriem J, LaFemina PC, Jónsson S, Bennett RA, Metzger S, Holland A, Sturkell E (2010) Overview of results from continuous GPS observations in Iceland from 1995 to 2010. *Jökull* 60:3–22
- Gíslason SR, Stefánsdóttir G, Pfeffer MA, Barsotti S, Jóhannsson Th, Galeczka I, Bali E, Sigmarsson O, Stefánsson A, Keller NS, Sigurdsson Á, Bergsson B, Galle B, Jacobo VC, Arellano S, Aiuppa A, Jónasdóttir EB, Eiríksdóttir ES, Jakósson S, Gudmundsson MT (2015) Environmental pressure from the 2014–15 eruption of Bárðarbunga volcano, Iceland. *Geochem Perspect Lett*. <https://doi.org/10.7185/geochemlet.1509>
- Gudmundsson MT, Jónsdóttir K, Hooper A, Holohan EP, Halldórsson SA, Ófeigsson BG, Cesca S, Vogfjörð KS, Sigmundsson F, Högnadóttir T (2016) Gradual caldera collapse at Bárðarbunga volcano, Iceland, regulated by lateral magma outflow. *Science* 353(6296):6296

- Gudmundsson MT, Larsen G, Höskuldsson Á, Gylfason ÁG (2008) Volcanic hazards in Iceland. *Jökull* 58:251–268
- Halldórsson SA, Marshall EW, Caracciolo A (2022) Rapid shifting of a deep magmatic source at Fagradalsfjall volcano, Iceland. *Nature* 609:529–534. <https://doi.org/10.1038/s41586-022-04981-x>
- Hjartardóttir ÁR, Dürig T, Parks MM, Drouin V, Eyjólfsson V, Reynolds A, Jensen EH, Óskarsson BV, Belart JM, Ruch J, Gies N, Pedersen GB, Einarsson P (in preparation). Pre-existing fractures and eruptive vent openings during the 2021 Fagradalsfjall eruption, Iceland.
- Hreinsdóttir S, Einarsson P, Sigmundsson F (2001) Crustal deformation at the oblique spreading Reykjanes Peninsula, SW Iceland: GPS measurements from 1993 to 1998. *J Geophys Res Solid Earth* 106(B7):13803–13816
- ICAO (2020) HANDBOOK ON THE INTERNATIONAL AIRWAYS VOLCANO WATCH (IAVW) [OPERATIONAL PROCEDURES AND CONTACT LIST]. <https://www.icao.int/airnavigation/METP/MOGVA%20Reference%20Documents/Handbook%20on%20the%20IAVW,%20Doc%209766.pdf>
- Icelandic Meteorological Office. (2022). Ekkert hraunflæði í þrjá mánuði við Fagradalsfjall. <https://www.vedur.is/um-vi/frettir/ekkert-hraunflaedi-i-thrja-manudi-vid-fagradalsfjall>
- Icelandic Tourism Dashboard. (2022). Number of tourists at Geldingadalir eruption. <https://www.maela.bordferdathjonustunnar.is/en/volcanic-eruption-in-geldingadalir>
- Ilyinskaya E, Schmidt A, Mather TA, Pope FD, Witham C, Baxter B, Jóhannsson T, Pfeffer M, Barsotti S, Singh A (2017) Understanding the environmental impacts of large fissure eruptions: aerosol and gas emissions from the 2014–2015 Holuhraun eruption (Iceland). *Earth Planet Sci Lett* 472:309–322
- Keiding M, Arnadóttir T, Jónsson S, Decriem J, Hooper A (2010) Plate boundary deformation and man-made subsidence around geothermal fields on the Reykjanes Peninsula, Iceland. *J Volcanol Geoth Res* 194(4):139–149
- Klein FW, Einarsson P, Wyss M (1973) Microearthquakes on Mid-Atlantic plate boundary on Reykjanes-peninsula in Iceland. *J Geophys Res* 78(23):5084–5099
- Klein FW, Einarsson P, Wyss M (1977) The Reykjanes Peninsula, Iceland, earthquake swarm of September 1972 and its tectonic significance. *J Geophys Res* 82(5):865–888
- Kullman GJ, Jones WG, Cornwell RJ, Parker JE (1994) Characterization of air contaminants formed by the interaction of lava and sea water. *Environ Health Perspect* 102(5):478–482
- Lowenstern J, Wallace K, Barsotti S, Sandri L, Stovall W, Bernard B, Privitera E, Komorowski J-C, Fournier N, Balagizi C (2022) Guidelines for volcano-observatory operations during crises: recommendations from the 2019 volcano observatory best practices meeting. *J Appl Volcanol* 11(1):1–24
- Mason E, Wieser PE, Liu EJ, Edmonds M, Ilyinskaya E, Whitty RC, Mather TA, Elias T, Nadeau PA, Wilkes TC (2021) Volatile metal emissions from volcanic degassing and lava–seawater interactions at Kīlauea Volcano, Hawai‘i *Commun Earth Environ* 2(1):1–16
- Mastin LG (2001) A simple calculator of ballistic trajectories for blocks ejected during volcanic eruptions. US Department of the Interior, US Geological Survey
- Pallister J, Papale P, Eichelberger J, Newhall C, Mandeville C, Nakada S, Marzocchi W, Loughlin S, Jolly G, Ewert J (2019) Volcano observatory best practices (VOBP) workshops—a summary of findings and best-practice recommendations. *J Appl Volcanol* 8(1):1
- Pedersen GB, Belart JM, Óskarsson BV, Gudmundsson MT, Gies N, Högnadóttir T, Hjartardóttir ÁR, Pinel V, Berthier E, Dürig T (2022) Volume, effusion rate, and lava transport during the 2021 Fagradalsfjall eruption: results from near real-time photogrammetric monitoring. *Geophys Res Lett* 49(13):e2021GL097125
- Pedersen GBM, Gudmundsson MT, Óskarsson B, Belart J, Gies N, Hognadóttir T, Hjartardóttir Á, Dürig T, Reynolds H, Valsson G, Hamilton C, Gunnarsson A, Pinel V, Berthier E, Einarsson P, Oddsson B (2021) Volume, Discharge Rate and Lava Transport at the Fagradalsfjall Eruption 2021: Results from Near-Real Time Photogrammetric Monitoring. American Geophysical Union, New Orleans. <https://agu.confex.com/agu/fm21/meetingapp.cgi/Paper/935003>
- Pedersen G, Höskuldsson A, Dürig T, Thordarson T, Jonsdóttir I, Riisshuus MS, Óskarsson BV, Dumont S, Magnússon E, Gudmundsson MT (2017) Lava field evolution and emplacement dynamics of the 2014–2015 basaltic fissure eruption at Holuhraun, Iceland. *J Volcanol Geoth Res* 340:155–169
- Pfeffer MA, Aiuppa A, Scott S, Stefánsson KR, Oppenheimer C, Edwards B, Hjörvar T, Bitetto M, Giudice G (In preparation). Ground-based gas measurements of the 2021a Fagradalsfjall eruption cloud
- Pfeffer MA, Arellano S, Petersen GN, Barnie T, Barsotti S, Bali E, Hjörvar T, Gudmundsson G, Vogfjörð K, Ilyinskaya E, Pedersen GB, Ranta E, Óladóttir BA, Edwards B, Moussallam Y, Stefánsson A, Scott S, Smekens J-F, Varnam M (In preparation). SO<sub>2</sub> emissions during the 2021b eruption of Fagradalsfjall, Iceland as measured by ground-based DOAS: A detailed analysis of emission rate

- variations during different eruption phases and eruptive behaviour and the impact of high-temporal emission rate variations on an air pollution dispersion forecast
- Pfeffer M, Bergsson B, Barsotti S, Stefánsdóttir G, Galle B, Arellano S, Conde V, Donovan A, Ilyinskaya E, Burton M (2018) Ground-based measurements of the 2014–2015 Holuhraun volcanic cloud (Iceland). *Geosciences* 8(1):1
- Sæmundsson K (1978) Fissure swarms and central volcanoes of the neovolcanic zones of Iceland in Crustal evolution in northern Britain and adjacent regions. *Geol J Liverp* 10:415–432
- Sæmundsson K, Sigurgeirsson MÁ (2013) Reykjaneskagi. In: Sólnes J, Sigmundsson F, Bessason B (eds) *Náttúruvá á Íslandi. Eldgos og Jarðskjálftar. Viðlagatrygging Íslands/Háskólaútgáfan*
- Sæmundsson K, Sigurgeirsson MÁ, Friðleifsson GÓ (2020) Geology and structure of the Reykjanes volcanic system, Iceland. *J Volcanol Geoth Res* 391:106501
- Scire JS, Strimaitis DG, Yamartino RJ (2000) A user's guide for the CALPUFF dispersion model. Earth Tech, Inc., Concord, MA, p 10
- Sigmundsson F, Einarsson P, Hjartardóttir ÁR, Drouin V, Jónsdóttir K, Arnadóttir T, Geirsson H, Hreinsdóttir S, Li S, Ófeigsson BG (2020) Geodynamics of Iceland and the signatures of plate spreading. *J Volcanol Geoth Res* 391:106436
- Sigmundsson F, Hooper A, Hreinsdóttir S, Vogfjörd KS, Ófeigsson BG, Heimisson ER, Dumont S, Parks M, Spaans K, Gudmundsson GB (2015) Segmented lateral dyke growth in a rifting event at Bárðarbunga volcanic system, Iceland. *Nature* 517(7533):7533
- Sigmundsson F, Parks MM, Hooper A, Geirsson H, Vogfjörd K, Drouin V, Ófeigsson BG, Hreinsdóttir S, Hjaltadóttir S, Jónsdóttir K, Einarsson P, Barsotti S, Horálek J, Ágústsdóttir T (2022) Deformation and seismicity decline preceding a rift zone eruption at Fagradalsfjall, Iceland. *Nature* 609:523–528. <https://doi.org/10.1038/s41586-022-05083-4>
- Soubestre J (in preparation). The Dynamics of the Fagradalsfjall 2021 Eruption Revealed by Volcanic Tremor Patterns
- Statistics in Iceland. (2022). Inhabitants. <https://www.statice.is/statistics/population/inhabitants/>
- Sturkell E, Einarsson P, Sigmundsson F, Geirsson H, Olafsson H, Pedersen R, de Zeeuw-van Dalfsen E, Linde AT, Sacks SI, Stefánsson R (2006) Volcano geodesy and magma dynamics in Iceland. *J Volcanol Geoth Res* 150(1–3):14–34
- Sturkell E, Sigmundsson F, Einarsson P, Bilham R (1994) Strain accumulation 1986–1992 across the Reykjanes Peninsula plate boundary, Iceland, determined from GPS measurements. *Geophys Res Lett* 21(2):125–128
- Tarquini S, de'Michieli Vitturi M, Jensen EH, Pedersen GB, Barsotti S, Coppola D, Pfeffer MA (2018) Modeling lava flow propagation over a flat landscape by using MrLavaLoba: The case of the 2014–2015 eruption at Holuhraun, Iceland
- Tryggvason E (1970) Surface deformation and fault displacement associated with an earthquake swarm in Iceland. *J Geophys Res* 75(23):4407–4422
- Whitty RC, Ilyinskaya E, Barsotti S, Pfeffer MA, Roberts T, Schmidt A, Jóhannsson TH, Gilbert G, Hjörvar T, Þrastarson R, Fecht D, Sigurðsson E, Sæmundsson G (in preparation). SO<sub>2</sub> and PM air quality and Icelandic population exposure during the 2021 Fagradalsfjall eruption

**Publisher's Note** Springer Nature remains neutral with regard to jurisdictional claims in published maps and institutional affiliations.

## Authors and Affiliations

S. Barsotti<sup>1</sup>  · M. M. Parks<sup>1</sup>  · M. A. Pfeffer<sup>1</sup>  · B. A. Óladóttir<sup>1</sup>  · T. Barnie<sup>1</sup>  ·  
M. M. Titos<sup>1,5</sup>  · K. Jónsdóttir<sup>1</sup>  · G. B. M. Pedersen<sup>2</sup>  · Á. R. Hjartardóttir<sup>2</sup>  ·  
G. Stefansdóttir<sup>1</sup>  · T. Johannsson<sup>3</sup> · P. Arason<sup>1</sup>  · M. T. Gudmundsson<sup>2</sup>  ·  
B. Oddsson<sup>4</sup>  · R. H. Þrastarson<sup>1</sup> · B. G. Ófeigsson<sup>1</sup>  · K. Vogfjörð<sup>1</sup>  · H. Geirsson<sup>2</sup>  ·  
T. Hjörvar<sup>1</sup> · S. von Löwis<sup>1</sup>  · G. N. Petersen<sup>1</sup>  · E. M. Sigurðsson<sup>1</sup>

M. M. Parks  
michelle@vedur.is

M. A. Pfeffer  
melissa@vedur.is

B. A. Óladóttir  
bergrun@vedur.is

T. Barnie  
talfan@vedur.is

M. M. Titos  
manuel@vedur.is

K. Jónsdóttir  
kristin.jonsdottir@vedur.is

G. B. M. Pedersen  
gro@hi.is

Á. R. Hjartardóttir  
astahj@hi.is

G. Stefansdóttir  
gerdur@vedur.is

T. Johannsson  
thorsteinnj@umhverfisstofnun.is

P. Arason  
arason@vedur.is

M. T. Gudmundsson  
mtg@hi.is

B. Oddsson  
bjorn.oddsson@logreglan.is

R. H. Þrastarson  
rhth@vedur.is

B. G. Ófeigsson  
bgo@vedur.is

K. Vogfjörð  
vogfjord@vedur.is

H. Geirsson  
hgeirs@hi.is

T. Hjörvar  
tryggvi@vedur.is

S. von Löwis  
sibylle@vedur.is

G. N. Petersen  
gnp@vedur.is

E. M. Sigurðsson  
eysteinn@vedur.is

- <sup>1</sup> Icelandic Meteorological Office, Reykjavík, Iceland
- <sup>2</sup> Earth Institute of Sciences, University of Iceland, Reykjavík, Iceland
- <sup>3</sup> Environment Agency of Iceland, Reykjavík, Iceland
- <sup>4</sup> Department of Civil Protection, Reykjavík, Iceland
- <sup>5</sup> University of Granada, Granada, Spain